Journal of Korean Society of
Coastal and Ocean Engineers
Vol. 15, No. 1, pp. 11~20, March 2003

On the Calculation of Irregular Wave Reflection from Perforated-Wall Caisson Breakwaters Using a Regular Wave Model
규칙파 모델을 이용한 유공케이슨 방파제로부터의 불규칙파 반사율 산정에 대하여

Kyung-Duck Suh* and Sang Young Son**
서경덕* · 손상영**

Abstract □ In this paper we examine several methods for calculating the reflection of irregular waves from a perforated-wall caisson breakwater using a regular wave model. The first method is to approximate the irregular waves as a regular wave whose height and period are the same as the root-mean-squared wave height and significant wave period, respectively, of the irregular waves. The second is to use the regular wave model, repeatedly, for each frequency component of the irregular wave spectrum. The wave period is determined according to the frequency of the component wave, and the root-mean-squared wave height is used for all the frequencies. The third method is the same as the second one except that the wave height corresponding to the energy of each component wave is used. Comparison with experimental data from previous authors shows the second method is the most adequate, giving reasonable agreement in both frequency-averaged reflection coefficients and reflected wave spectra.

Keywords : irregular waves, laboratory tests, perforated-wall caisson breakwaters, regular wave models, water waves, wave reflection

要 旨 : 본 논문에서는 규칙파 모델을 이용하여 유공케이슨 방파제로부터의 불규칙파의 반사를 계산하는 몇 가지 방법들을 검토한다. 첫번째 방법은 불규칙파를 파고 및 주기가 각각 불규칙파의 제곱평균제곱근 파고 및 유의주기와 같은 규칙파로 근사하는 것이다. 두 번째는 불규칙파 스펙트럼의 각 주파수 성분에 대하여 규칙파 모델을 반복적으로 사용하는 것이다. 파의 주기는 성분파의 주파수에 따라 결정되며, 모든 주파수에 대해서 제곱평균제곱근 파고를 사용한다. 세 번째 방법은 두 번째 방법과 같으나, 각 성분파의 에너지에 해당하는 파고를 사용한다. 이전 연구자들의 실험 결과와 비교해 본 결과, 두 번째 방법이 가장 타당하며, 주파수 평균 반사율과 반사파 스펙트럼 모두 실험치와 양호한 일치를 보였다.

핵심용어 : 불규칙파, 실험실 실험, 유공케이슨 방파제, 규칙파 모델, 파랑, 파의 반사

1. Introduction

A perforated-wall caisson is often used to remedy drawbacks with conventional vertical-wall caisson. It reduces not only wave reflection but also wave transmission due to overtopping. It also reduces wave forces, especially impulsive wave forces, acting on the caisson (Takahashi and Shimosako, 1994; Takahashi *et al.*, 1994). Numerous theoretical and experimental studies have been performed to investigate its hydraulic and hydrodynamic characteristics.

*서울대학교 지구환경시스템공학부 및 해양시스템공학연구소(School of Civil, Urban, and Geosystem Engineering & Research Institute of Marine Systems Engineering, Seoul National University, San 56-1, Shinlim-Dong, Gwanak-Gu, Seoul 151-742, Korea. kdsuh@snu.ac.kr)
**현대건설주식회사 기술연구소 토목기술부(Hyundai Institute of Construction Technology, Hyundai Engineering & Construction Co., Ltd.)

Hydraulic model tests have been used to examine the reflection characteristics of a perforated-wall caisson breakwater (Jarlan, 1961; Marks and Jarlan, 1968; Terret *et al.*, 1968; Tanimoto *et al.*, 1976; Bennett *et al.*, 1992; Park *et al.*, 1993). Efforts have also been made toward developing analytical models for predicting the reflection coefficient (Kondo, 1979; Kakuno *et al.*, 1992; Bennett *et al.*, 1992; Fugazza and Natale, 1992; Suh and Park, 1995). The previous studies used analytical models developed for regular waves, though they include several experimental studies that dealt with irregular waves [e.g., Tanimoto *et al.* (1976) and Bennett *et al.* (1992)]. Very recently, Suh *et al.* (2001) developed an analytical model that predicts the reflection of irregular waves from a perforated-wall caisson. They also conducted laboratory experiments involving irregular waves, of various significant wave heights and periods, impinging upon perforated-wall caissons with various wave chamber widths. The experimental results were compared with the analytical model for frequency-averaged reflection coefficients as well as reflected wave spectra.

Although irregular wave models such as the Suh *et al.*'s (2001) model become available, regular wave models are still in extensive use due to their simplicity. There are several ways to calculate the reflection of irregular waves using a regular wave model. One is to approximate the irregular waves as a regular wave whose height and period are the same as the root-mean-squared (abbreviated as rms hereinafter) wave height and significant wave period, respectively, of the irregular waves [e.g., Suh and Park (1995)]. This method is referred to as Method 1 in this study. This method inherently assumes that the reflection coefficient is constant for all the frequency component of the irregular waves, so the frequency dependent nature of wave reflection cannot be examined. Another way is to use the regular wave model, repeatedly, for each frequency component of the irregular wave spectrum [e.g., Bennett *et al.* (1992)]. The wave period is determined according to the frequency of the component wave, but it is questionable what wave height should be used. Either the rms wave height could be used for all the frequencies, or the wave height corresponding to the energy of each component wave could be used at each frequency. The former is referred to as Method 2, and the latter as Method 3.

In this study, we examine the adequacy of the above-mentioned methods by comparing the calculated results with the available experimental data of irregular waves. We use the regular wave model developed by Fugazza and Natale (1992). Even though this model has been validated using the experimental work of previous authors, we carried out laboratory experiments to re-validate the model. In the following section, the analytical model of Fugazza and Natale (1992) is briefly summarized. In section 3, the laboratory experiments for regular waves are described. In section 4, the regular wave experimental data are compared with the analytical model. In section 5, the regular wave model is applied to calculate the irregular wave reflection from the experiments of Suh *et al.* (2001) and Bennett *et al.* (1992). The major conclusions then follow.

2. Description of the regular wave model

Let us consider the perforated-wall caisson breakwater with vertical slits, as sketched in Fig. 1, where h is the constant water depth in still water, and B is the wave chamber width. The distance between the centers of two adjacent members of the slit wall is denoted as $2A$, and the width of a slit as $2a$, so that the porosity of the wall is $r = a/A$. The thickness of the wall is denoted as d. The x-axis and y-axis are taken to be normal, and parallel, to the crest line of the wall respectively. The vertical coordinate z is measured vertically from the still water line. Consider monochro-

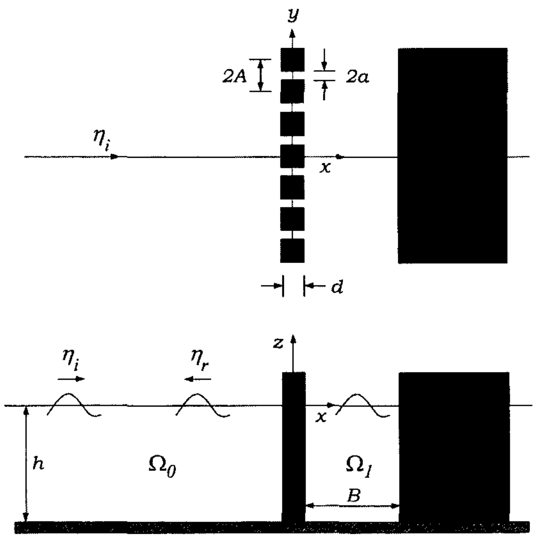

Fig. 1. Schematic diagram and coordinate system for calculation of wave reflection.

matic, long-crested, and small-amplitude waves, with the wave height H, normally incident on the breakwater. The wave number of the incident wave is denoted as $k = 2\pi/L$, where L is the wavelength. The linear dispersion relationship is given by $\omega^2 = gk\tanh kh$, where ω is the angular frequency, and g the gravitational acceleration.

Neglecting the evanescent waves, the wave potential in the region $\Omega_j (j = 0, 1)$ is expressed as

$$\Phi_j = \mathrm{Re}\{(a_j + ib_j)\cosh[k(z+h)]e^{i(kx-\omega t)} + (c_j + id_j)\cosh[k(z+h)]e^{i(kx+\omega t)}\} \tag{1}$$

where $i = \sqrt{-1}$, $a_0 = gH/(2\omega\cosh kh)$, and $b_0 = 0$.

At the solid back wall located at $x = B$, the no-flux condition must be satisfied:

$$\frac{\partial\Phi_1}{\partial x} = 0 \tag{2}$$

At the perforated wall, $x = 0$, the following matching conditions must be satisfied:

$$\frac{\partial\Phi_0}{\partial x} - \frac{\partial\Phi_1}{\partial x} = 0 \tag{3}$$

$$\frac{\partial\Phi_1}{\partial t} - \frac{\partial\Phi_0}{\partial t} - \beta\frac{\partial\Phi_0}{\partial x} - l\frac{\partial^2\Phi_0}{\partial x\partial t} = 0 \tag{4}$$

Here l is the length of the jet flowing through the slit, and β is the linearized dissipation coefficient given by

$$\beta = \frac{8\alpha}{9\pi}H\omega\frac{W}{\sqrt{W^2(R+1)^2 + G^2}}\frac{5+\cosh 2kh}{2kh+\sinh 2kh} \tag{5}$$

where $W = \tan(kB)$, $R = \beta k/\omega$, $P = lk$, $G = 1 - PW$, and $\alpha = [1/(rC_c) - 1]^2$ is the energy loss coefficient with C_c being the empirical contraction coefficient at the slit. Mei *et al.* (1974) suggest using the formula

$$C_c = 0.6 + 0.4r^2 \tag{6}$$

for a rectangular geometry like a vertical slit. Note that R in Eq. (5) is a function of β. Rearranging Eq. (5) gives a quartic polynomial of β, which can be solved by the eigenvalue method (see Press *et al.*, 1992, p. 368).

Substitution of Eq. (1) with $j = 0$ and 1 into Eqs. (2) to (4) yields a system of linear equations in the unknowns, c_0, d_0, a_1, b_1, c_1, and d_1. Solving these equations, we get

$$c_0 = a_0\frac{G^2 - W^2(1-R^2)}{G^2 + W^2(1+R^2)} \tag{7}$$

$$d_0 = -a_0\frac{2GW}{G^2 + W^2(1+R^2)} \tag{8}$$

Finally the reflection coefficient is obtained as

$$C_r = \frac{\sqrt{c_0^2 + d_0^2}}{a_0} = \frac{[(G^2+W^2)^2 + W^2R^2(W^2R^2 + 2G^2 - 2W^2)]^{1/2}}{G^2 + W^2(1+R^2)} \tag{9}$$

In Eq. (4), the jet length, l, represents the inertial resistance at the perforated wall. Fugazza and Natale (1992) assumed that the importance of the local inertia term is weak, and they took the jet length to be equal to the wall thickness, d. On the other hand, Kakuno and Liu (1993) proposed a blockage coefficient to represent the inertial resistance:

$$C = \frac{d}{2}\left(\frac{A}{a} - 1\right) + \frac{2A}{\pi}\left[1 - \log\left(\frac{4a}{A}\right) + \frac{1}{3}\left(\frac{a}{A}\right)^2 + \frac{281}{180}\left(\frac{a}{A}\right)^4\right] \tag{10}$$

Comparison of the Fugazza and Natale (1992) and Kakuno and Liu (1993) models gives

$$l = 2C \tag{11}$$

which is much greater than the wall thickness, d, implying the influence of the inertial resistance term is not so insignificant. For example, when $d = 1$ cm, $A = 3$ cm, and $a = 1$ cm, the jet length, l, is calculated to be 5.84 cm using the preceding equations, which is almost 6 times the wall thickness. In this study, Eq. (11) is used to calculate the jet length, because it gives better agreement, with the experimental data, than assuming that $l = d$.

In Methods 2 and 3 described in the introduction, the reflection coefficient is calculated differently for each frequency component. The spectral density of the reflected waves is calculated for a particular frequency component by

$$S_{\eta,r}(f) = |C_r(f)|^2 S_{\eta,i}(f) \tag{12}$$

where f is the wave frequency and $S_{\eta,i}(f)$ is the incident wave energy spectrum. The frequency-averaged reflection coefficient is then calculated as (Goda, 2000)

$$\overline{C}_r = \sqrt{\frac{m_{0,r}}{m_{0,i}}} \tag{13}$$

where $m_{0,i}$ and $m_{0,r}$ are the zeroth moments of the incident and reflected wave spectra, respectively, obtained by integrating each spectrum over the entire frequency range.

Table 1. Experimental conditions and analyzed data

B (cm)	H (cm)	T (s)	H^m (cm)	T^m (s)	C_r^c	C_r^m	Error (%)
15	3	1.0	3.00	0.99	0.701	0.690	1.6
	3	1.2	2.87	1.15	0.848	0.817	3.6
	3	1.4	3.06	1.33	0.913	0.891	2.4
	3	1.6	2.98	1.54	0.952	0.930	2.3
	3	1.8	3.11	1.70	0.965	0.908	6.0
	3	2.0	3.09	1.91	0.977	0.861	11.9
	6	1.2	6.18	1.19	0.764	0.724	5.2
	6	1.4	5.80	1.40	0.875	0.862	1.5
	6	1.6	5.77	1.60	0.923	0.896	3.0
	6	1.8	5.89	1.78	0.946	0.927	2.0
	6	2.0	6.10	1.94	0.959	0.886	7.6
	9	1.4	8.94	1.39	0.821	0.816	0.7
	9	1.6	8.99	1.60	0.888	0.851	4.2
	9	1.8	8.74	1.80	0.926	0.888	5.1
	9	2.0	8.67	2.00	0.948	0.868	8.5
30	3	1.0	2.96	0.99	0.365	0.384	−5.3
	3	1.2	3.00	1.15	0.482	0.550	−14.0
	3	1.4	3.11	1.33	0.613	0.692	−12.8
	3	1.6	3.13	1.54	0.731	0.729	0.2
	3	1.8	3.02	1.70	0.799	0.799	0.1
	3	2.0	3.02	1.91	0.856	0.823	3.8
	6	1.2	6.01	1.19	0.329	0.328	0.2
	6	1.4	5.78	1.40	0.516	0.515	0.2
	6	1.6	6.01	1.60	0.630	0.628	2.4
	6	1.8	6.06	1.78	0.709	0.692	2.4
	6	2.0	6.20	1.94	0.761	0.741	2.6
	9	1.4	11.65	1.39	0.384	0.427	−11.2
	9	1.6	9.15	1.60	0.548	0.560	−2.2
	9	1.8	8.81	1.80	0.649	0.654	−0.7
	9	2.0	8.64	2.00	0.725	0.694	4.3
45	3	1.0	2.92	0.99	0.548	0.549	−0.2
	3	1.2	2.93	1.15	0.420	0.435	−3.6
	3	1.4	3.08	1.33	0.422	0.461	−9.3
	3	1.6	3.13	1.54	0.510	0.552	−8.2
	3	1.8	3.12	1.70	0.584	0.656	−12.3
	3	2.0	3.09	1.91	0.669	0.665	0.6
	6	1.2	6.13	1.19	0.168	0.194	−15.6
	6	1.4	5.90	1.40	0.252	0.291	−15.3
	6	1.6	6.09	1.60	0.362	0.384	−6.2
	6	1.8	6.05	1.78	0.457	0.496	−8.4
	6	2.0	6.27	1.94	0.521	0.547	−5.0
	9	1.4	9.02	1.39	0.143	0.220	−53.8
	9	1.6	9.31	1.60	0.275	0.297	−8.0
	9	1.8	9.10	1.80	0.383	0.399	−4.0
	9	2.0	8.82	2.00	0.477	0.489	−2.6
60	3	1.0	2.88	0.99	0.891	0.873	2.0
	3	1.2	2.88	1.15	0.613	0.595	3.0
	3	1.4	3.04	1.33	0.448	0.457	−1.9

Table 1. continued

B (cm)	H (cm)	T (s)	H^m (cm)	T^m (s)	C_r^c	C_r^m	Error (%)
	3	1.6	3.14	1.54	0.411	0.416	−1.2
	3	1.8	2.93	1.70	0.465	0.486	−4.4
	3	2.0	3.05	1.91	0.518	0.531	−2.5
	6	1.2	6.02	1.19	0.377	0.374	0.9
	6	1.4	5.81	1.40	0.215	0.259	−20.3
	6	1.6	6.06	1.60	0.206	0.249	−20.9
	6	1.8	6.05	1.78	0.274	0.292	−6.8
	6	2.0	6.16	1.94	0.336	0.363	−8.1
	9	1.4	8.93	1.39	0.097	0.152	−56.0
	9	1.6	9.11	1.60	0.085	0.167	−95.6
	9	1.8	8.87	1.80	0.192	0.211	−9.7
	9	2.0	8.74	2.00	0.285	0.305	−7.0

Note that the reflection coefficient calculated by Method 1, as the ratio of the reflected rms wave height to the incident one, is equivalent to the frequency-averaged reflection coefficient because the rms wave height is proportional to $\sqrt{m_0}$.

3. Laboratory experiment for regular wave reflection

Experiments were carried out in the wave flume at the Breakwater Laboratory of the Korea Institute of Construction Technology. The flume was 56-m long, 2-m high, and 1-m wide. It was equipped with a piston-type wave generator at one end, and a wave-absorbing beach at the other. Wave generation and data acquisition were controlled using a personal computer. Water surface displacements were measured with parallel-wire capacitance-type wave gauges.

All the experiments were carried out at a water depth of 40 cm. The breakwater model was made from acrylic plates of 1 cm thickness, and the perforated wall consisted of vertical slits with $a = 1$ cm, $A = 3$ cm, and $d = 1$ cm, so that its porosity was 0.333. Four different wave chamber widths were used; 15, 30, 45, and 60 cm. The breakwater model was placed at a distance of 25 m from the wave maker.

Three different wave heights were used for each wave chamber width, with 4 to 6 different wave periods for each wave height. The target and measured (indicated by the superscript m) values of the incident wave heights and periods, along with the measured and calculated reflection coefficients, are given in Table 1.

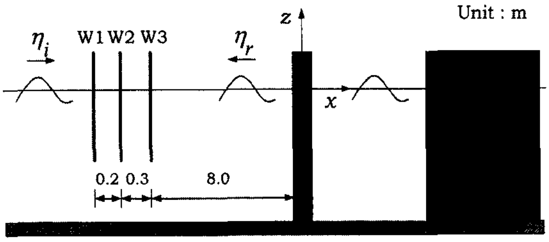

Fig. 2. Arrangement of wave gauges for measuring incident and reflected waves.

In order to measure the incident and reflected waves, three wave gauges were installed as shown in Fig. 2. The wave records measured at W1 to W3 were used to separate the incident and reflected waves using the technique developed by Park et al. (1992). Wave measurements were made for 300 s at a sampling rate of 20 Hz immediately after the initiation of wave generation. For the separation of incident and reflected waves, we had to use the wave records that included the incident waves and the reflected waves from the breakwater, but did not include the re-reflected waves from the wave paddle. The leading wave propagates at the speed of the group velocity. Therefore, the time for the leading wave generated by the wave maker to be reflected from the breakwater and arrive at the location of the wave gauges can be calculated approximately. By examining the plotted wave records and using the approximate arrival time of the first reflected wave, we selected a fraction of the wave records, for length of 10 wave periods, including only the incident waves and the reflected waves from the breakwater. This was then used for the separation of incident and reflected waves.

4. Validation of the regular wave model

In this section, comparing the computational results with the experimental measurements is used to validate the regular wave model. The measured and calculated reflection coefficients, along with the relative error, are given in Table 1. The relative error was calculated using

$$\text{Error} = \frac{C_r^c - C_r^m}{C_r^c} \times 100\% \tag{14}$$

where the superscripts, c and m, denote calculation and measurement, respectively. The contraction coefficient, C_c, was calculated to be 0.644 from Eq. (6), but a slight

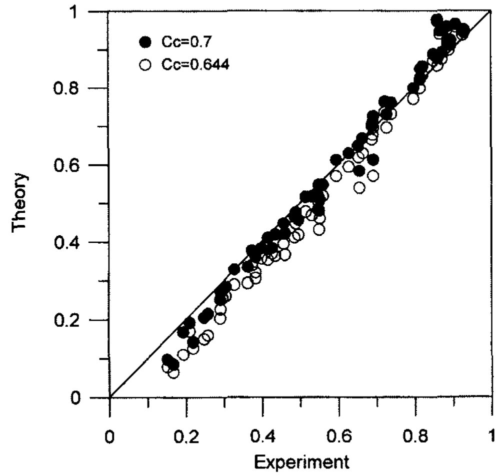

Fig. 3. Comparison of regular wave reflection coefficients between experiment and theory.

improvement was obtained using C_c=0.7 instead, as shown in Fig. 3. Therefore, C_c=0.7 was used in the computational results presented hereinafter. The reflection coefficients in Table 1 were also calculated using C_c=0.7.

Comparison of the measured and calculated reflection coefficients is shown in Fig. 3. The results when C_c=0.7 show slightly better agreement than those when C_c=0.644. Although the overall agreement is acceptable when we used C_c=0.7, the model over-predicted the reflection coefficients at larger values, while under-predicted them at smaller values. These differences may be attributed to the neglect of the evanescent waves near the breakwater (Park *et al.*, 2000; Suh *et al.*, 2001).

5. Calculation of irregular wave reflection using the regular wave model

5.1 Comparison with the Suh *et al.*'s experimental data

Suh *et al.* (2001) carried out laboratory experiments, for irregular wave reflection from perforated-wall caisson breakwaters, using the same breakwater models and wave flume as those used in this study. The incident wave spectrum used in the experiment was the Bretschneider-Mitsuyasu spectrum given by

$$S_{\eta,i}(f) = 0.205 H_s^2 T_s (T_s f)^{-5} \exp[-0.75 (T_s f)^{-4}] \tag{15}$$

where H_s and T_s are the significant wave height and period, respectively. They used target significant wave

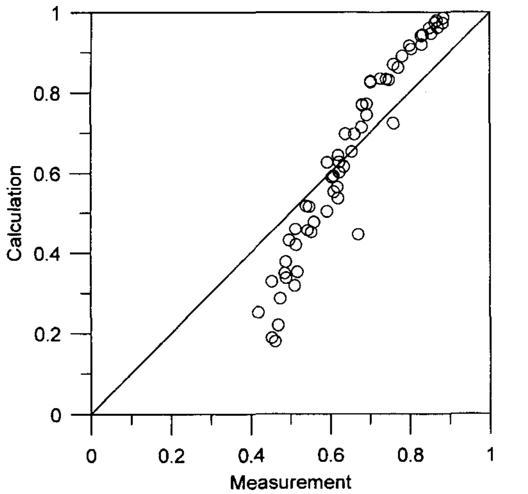

Fig. 4. Comparison of frequency-averaged reflection coefficients between measurement and calculation by Method 1.

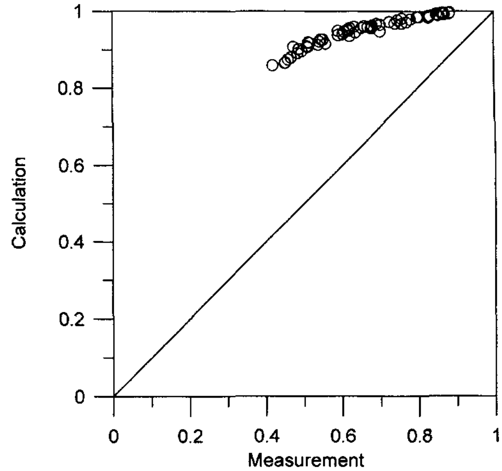

Fig. 6. Same as Fig. 4, but for Method 3.

heights and periods that were the same as the target values of the regular waves in Table 1. In the following calculation, however, the measured values of significant wave heights and periods (or the measured incident wave spectrum) are used.

Fig. 4 shows a comparison of the frequency-averaged reflection coefficients between measurement and calculation by Method 1. The model considerably over-predicted the reflection coefficients at larger values, while largely under-predicted them at smaller values. Fig. 5 shows the results from Method 2. Though the model somewhat over-predicted the reflection coefficients at larger values, the overall agreement was acceptable. Fig. 6 shows the results from Method 3. The model severely over-predicted the reflection coefficients because the energy dissipation at the perforated wall, which is proportional to the wave height, is calculated to be very small so most of the wave energy is reflected from the breakwater. Note that the wave height corresponding to the energy of each component wave, from Method 3, is much smaller than the rms wave height used in Method 2.

To examine the frequency-dependent nature of wave

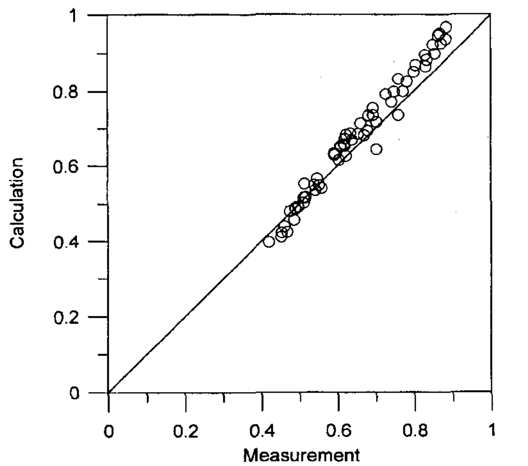

Fig. 5. Same as Fig. 4, but for Method 2.

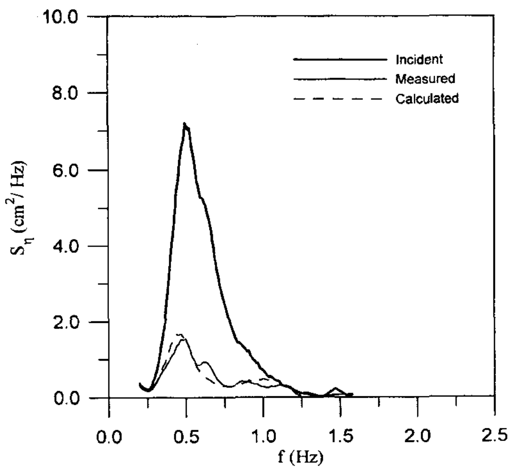

Fig. 7. Measured and calculated spectra of incident and reflected waves for the case of $H_s = 6$ cm, $T_s = 1.8$ s, and $B = 60$ cm: thick solid line = incident wave, thin solid line = measured reflected wave, thin dashed line = calculated reflected wave.

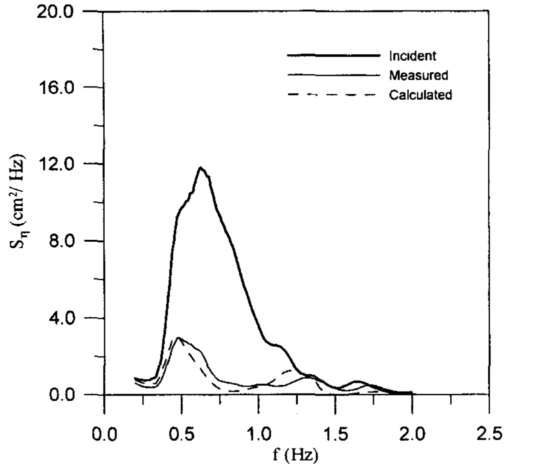

Fig. 8. Same as Fig. 7, but for $H_s = 9$ cm, $T_s = 1.4$ s, and $B =$ 45 cm.

reflection in detail, the measured incident and reflected wave spectra were plotted, along with the spectrum calculated from Method 2. The two cases, which gave the best and worst agreement between measured and calculated frequency-averaged reflection coefficient, are presented in Figs. 7 and 8, respectively. Similar plots for other experimental conditions can be found in Son (2002). In these figures, the thick solid line indicates the measured incident wave spectrum, while the thin solid and dashed lines indicate the measured and calculated reflected wave spectra, respectively. Fig. 7 shows the results for the case where $H_s \approx 6$ cm, $T_s \approx 1.8$ s and $B = 60$ cm, for which the error calculated by Eq. (14) for the frequency-averaged reflection coefficient is 0.02%. Although it is almost error-free in terms of the frequency-averaged reflection coefficient, the details of the spectra show some difference. Fig. 8, on the other hand, shows the results for the case where $H_s \approx 9$ cm, $T_s \approx 1.4$ s and $B = 45$ cm, for which the error is −10.1%. The details show some difference depending on the frequency, but the overall agreement is still acceptable.

5.2 Comparison with the Bennett *et al.*'s experimental data

The laboratory experiments of Suh *et al.* (2001) were only small scale. On a relatively larger scale, 1:15, Bennett *et al.* (1992) carried out laboratory experiments for irregular wave reflection from a slotted wave screen breakwater with, and without, a solid back wall. Here, we utilized the

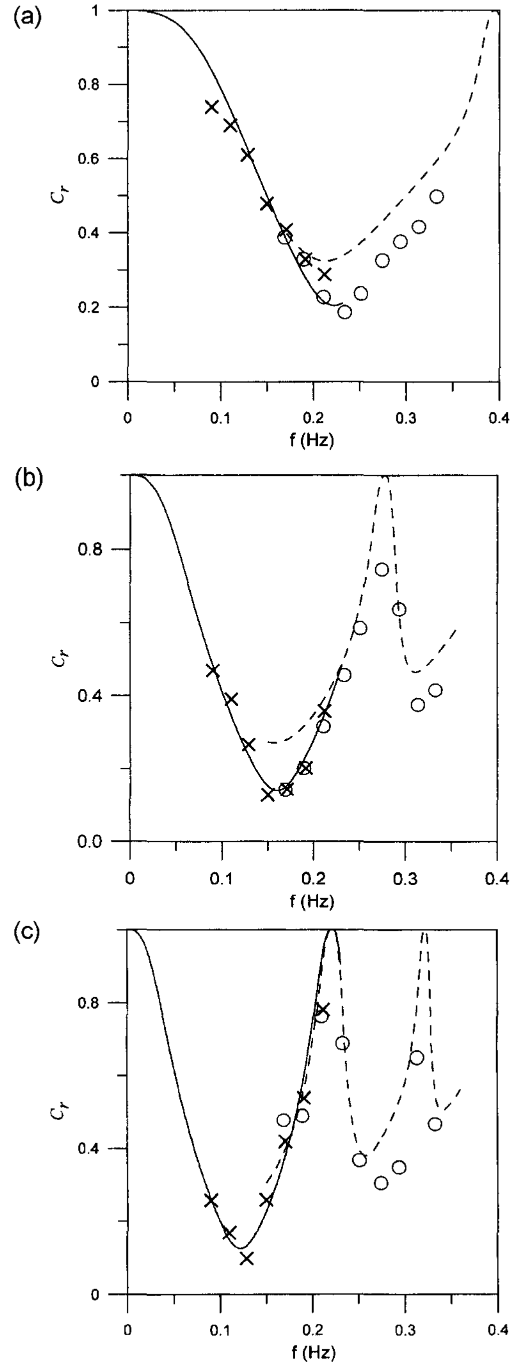

Fig. 9. Reflection coefficient versus frequency for a constant porosity of slit wall ($r = 0.148$) and varying wave chamber widths: solid line = calculation for spectrum A, dashed line = calculation for spectrum B, × = measurement of spectrum A, ○= measurement of spectrum B. (a) $B = 5$ m, (b) $B = 10$ m, (c) $B =$ 15 m.

experimental data for the cases with a back wall. The experimental conditions, for the prototype, are given below. All the tests were carried out at a water depth of 8.6 m for two spectra. Spectrum A covered frequencies equivalent to wave periods of 4.5 to 14 s, and spectrum B covered those of 2.9 to 6.2 s. Significant wave heights, corresponding to spectra A and B, were 0.91 and 1.41 m, respectively. Three different wave chamber widths were used; 5, 10 and 15 m. Three different porosities of the slit wall were used for each spectrum; 0.209, 0.148 and 0.072. The geometric details of the slit wall were not described in the paper of Bennett *et al.* (1992). Therefore we assumed reasonable values, i.e., $A = 0.6$ m and $d = 15$ cm. The half width of a slit, a, is then determined depending on the porosity.

Method 2 was proven the most reasonable when compared with Suh *et al.*'s experimental data. Thus, only this method was examined. Fig. 9 shows the comparison between measured and calculated reflected wave spectra for a fixed porosity and various wave chamber widths. Though the model somewhat over-predicted the wave reflection at some frequencies for spectrum B, reasonable agreement was found over the entire frequency range. The reflected wave spectra in Fig. 9 show the frequency dependent oscillatory behavior. Without the inertial resistance at the slit wall, the minimum reflection would occur at $B/L=0.25$, which corresponds to

$$f = \sqrt{\frac{g}{8\pi B}\tanh\left(\frac{\pi h}{2B}\right)} \tag{16}$$

The frequencies of minimum reflection for B equal to 5, 10, and 15 m, were calculated to be 0.278, 0.185, and 0.136 Hz, respectively, from the preceding equation. In Fig. 9, however, the minimum reflection occurs at frequencies of about 0.22, 0.16, and 0.12 Hz, which correspond to B/L equal to 0.164, 0.204, and 0.214, respectively. The inertial resistance makes the minimum reflection to occur at the value of B/L somewhat smaller than 0.25. Previous authors have reported similar results.

Fig. 10 shows the results for a fixed wave chamber width but varying porosities of the slit wall. As the porosity decreases, the curves show sharper peaks and flatter troughs, and overall reflection increases.

The frequency-averaged reflection coefficients, and the relative errors calculated using Eqs. (13) and (14), respectively, are listed in Table 2. Good agreement between theory and experiment was found in all the cases for spectrum A, while the model somewhat over-predicted the reflection coefficients for spectrum B.

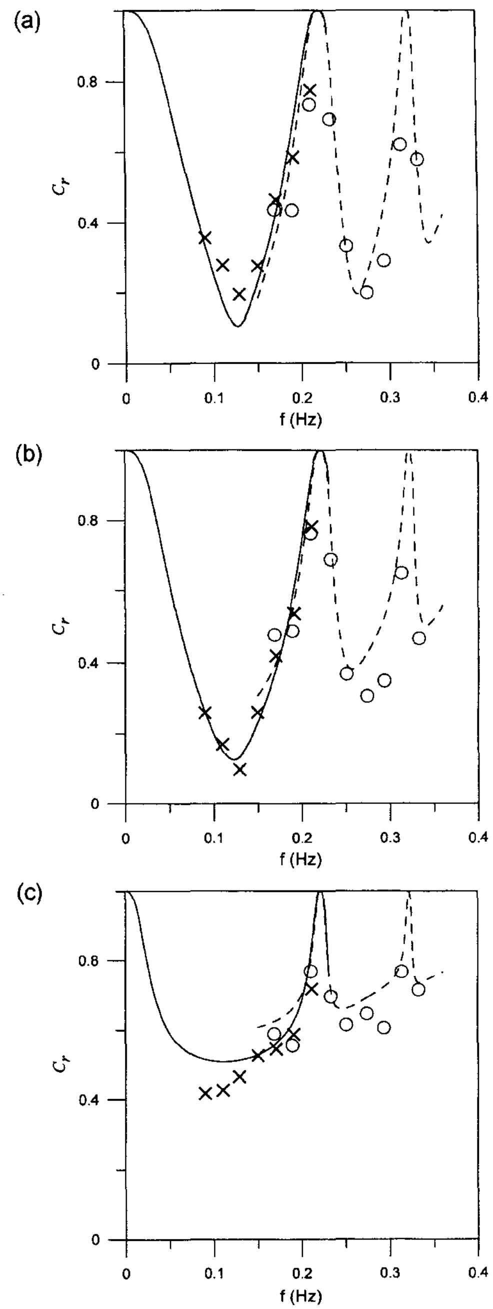

Fig. 10. Same as Fig. 9, but for a constant wave chamber width ($B = 15$ m) and varying porosity of slit wall. (a) $r = 0.209$, (b) $r = 0.148$, (c) $r = 0.072$.

Table 2. Frequency-averaged reflection coefficients of Bennett *et al.*'s (1992) experiment

Fig. No.	Chamber width (m)	porosity	Spectrum A			Spectrum B		
			Exp.	Theory	Error (%)	Exp.	Theory	Error (%)
9a	5	0.148	0.558	0.586	4.7	0.289	0.377	23.2
9b	10	0.148	0.307	0.301	−1.9	0.443	0.532	16.8
9c	15	0.148	0.366	0.394	7.1	0.569	0.646	11.9
10a	15	0.209	0.415	0.434	4.3	0.542	0.671	19.3
10b	15	0.148	0.366	0.394	7.1	0.569	0.646	11.9
10c	15	0.072	0.511	0.566	9.8	0.657	0.708	7.2

6. Summary and conclusions

In this study, three different methods were examined for calculating the irregular wave reflection from a perforated-wall caisson breakwater using a regular wave model. Method 1 approximates the irregular waves as a regular wave whose height and period are the same as the rms wave height and significant wave period, respectively, of the irregular waves. Method 2 uses the regular wave model, repeatedly, for each frequency component of the irregular wave spectrum with the rms wave height for all the frequencies. Method 3 is the same as Method 2 except the wave height corresponding to the energy of each component wave is used at each frequency.

Method 1 was found to considerably over-predict the frequency-averaged reflection coefficients at larger values, and mainly under-predict them at smaller values. This method inherently assumes that the reflection coefficient is constant for all the frequency components of the irregular waves, so the frequency dependent nature of wave reflection cannot be examined. Method 2 gave reasonable agreement with the experimental data in both frequency-averaged reflection coefficients and the reflected wave spectra, although it somewhat over-predicted the frequency-averaged reflection coefficients at larger values. This was probably because the model neglects the effect of evanescent waves near the breakwater. Method 3 severely over-predicted the reflection coefficients because the energy dissipation at the perforated wall, which is proportional to the wave height, was calculated to be very small so that most wave energy was reflected from the breakwater.

Concluding, Method 2 seems to be the most adequate if we use a regular wave model to predict the irregular wave reflection from a perforated-wall caisson breakwater. Method 1 that uses the most conventional approximation of irregular waves and has been widely used because of its simplicity gave large errors even in the frequency-averaged reflection coefficients, leaving aside the fact that it cannot resolve the frequency-dependent nature of wave reflection.

Acknowledgement

This work was supported by the Brain Korea 21 Project. We would also like to thank the Korea Institute of Construction Technology for allowing us to use the wave flume.

References

Bennett, G.S., McIver, P., and Smallman, J.V., 1992. A mathematical model of a slotted wavescreen breakwater, *Coastal Engineering*, **18**, pp. 231-249.

Fugazza, M. and Natale, L., 1992. Hydraulic design of perforated breakwaters, *Journal of Waterway, Port, Coastal and Ocean Engineering*, **118**, pp. 1-14.

Goda, Y., 2000. *Random Seas and Design of Maritime Structures*, 2nd ed., World Scientific, Singapore.

Jarlan, G.E., 1961. A perforated vertical wall breakwater, *Dock Harbour Authority*, **XII**(486), pp. 394-398.

Kakuno, S. and Liu, P.L.-F., 1993. Scattering of water waves by vertical cylinders, *Journal of Waterway, Port, Coastal and Ocean Engineering*, **119**, pp. 302-322.

Kakuno, S., Oda, K., and Liu, P.L.-F., 1992. Scattering of water waves by vertical cylinders with a backwall, *Proceedings of 23rd International Conference on Coastal Engineering*, ASCE, Venice, pp. 1258-1271.

Kondo, H., 1979. Analysis of breakwaters having two porous walls, *Proceedings of International Conference on Coastal Structures 79*, pp. 962-977.

Marks, M. and Jarlan, G.E., 1968. Experimental study on a fixed perforated breakwater, *Proceedings of 11th Interna-*

tional Conference on Coastal Engineering, ASCE, London, pp. 1121-1140.

Mei, C.C., Liu, P.L.-F., and Ippen, A.T., 1974. Quadratic loss and scattering of long waves, *Journal of Waterways, Harbors and Coastal Engineering Division*, ASCE, **100**, pp. 217-239.

Park, W.S., Chun, I.S., and Lee, D.S., 1993. Hydraulic experiments for the reflection characteristics of perforated breakwaters, *Journal of Korean Society of Coastal and Ocean Engineers*, **5**, pp. 198-203 (in Korean).

Park, W.S., Kim, B.H., Suh, K.D., and Lee, K.S., 2000. Scattering of irregular waves by vertical cylinders, *Coastal Engineering Journal*, **42**, pp. 253-271.

Park, W.S., Oh, Y.M., and Chun, I.S., 1992. Separation technique of incident and reflected waves using least squares method, *Journal of Korean Society of Coastal and Ocean Engineers*, **4**, pp. 139-145 (in Korean).

Press, W.H., Teukolsky, S.A., Vetterling, W.T., and Flannery, B.P., 1992. *Numerical Recipes in FORTRAN: The Art of Scientific Computing*, 2nd ed., Cambridge University Press.

Son, S.Y., 2002. *Calculation of irregular wave reflection from perforated-wall caisson breakwaters using a regular wave model*, Master thesis, Seoul National University, Seoul, Korea.

Suh, K.D., Choi, J.C., Kim, B.H., Park, W.S., and Lee, K.S., 2001. Reflection of irregular waves from perforated-wall caisson breakwaters, *Coastal Engineering*, **44**, pp. 141-151.

Suh, K.D. and Park, W.S., 1995. Wave reflection from perforated-wall caisson breakwaters. *Coastal Engineering*, **26**, pp. 177-193.

Takahashi, S. and Shimosako, K., 1994. Wave pressure on a perforated caisson, *Proceedings of Hydro-Port94*, Port and Harbour Research Institute, Yokosuka, Japan, pp. 747-764.

Takahashi, S., Tanimoto, K., and Shimosako, K., 1994. A proposal of impulsive pressure coefficient for the design of composite breakwaters, *Proceedings of Hydro-Port94*, Port and Harbour Research Institute, Yokosuka, Japan, pp. 489-504.

Tanimoto, K., Haranaka, S., Takahashi, S., Komatsu, K., Todoroki, M., and Osato, M., 1976. *An experimental investigation of wave reflection, overtopping and wave forces for several types of breakwaters and sea walls*, Technical Note of Port and Harbour Research Institute, Japan, No. 246 (in Japanese).

Terret, F.L., Osorio, J.D.C., and Lean, G.H., 1968. Model studies of a perforated breakwater. *Proceedings of 11th International Conference on Coastal Engineering*, ASCE, London, pp. 1104-1120.

Received November 5, 2002
Accepted December 11, 2002